Electronic Supplementary Material (ESI) for Journal of Materials Chemistry C.

Supplementary Information

Efficient tuning of the conversion from ISC to high-level RISC via adjusting the triplet energies of charge-transporting layers in rubrene-doped OLEDs

Xiantong Tang,[a] *Xi Zhao,*[a] *Hongqiang Zhu,*[b] *Linyao Tu,*[a] *Caihong Ma,*[a] *Ying Wang,*[a] *Shengnan Ye,*[a] *and Zuhong Xiong**[a]

[a]*School of Physical Science and Technology, MOE Key Laboratory on Luminescence and Real-Time Analysis, Southwest University, Chongqing 400715, China*

[b]*Chongqing Key Laboratory of Photo-Electric Functional Materials, Chongqing Normal University, Chongqing 401331, China*

Corresponding Author:

zhxiong@swu.edu.cn

Table S1. Energy levels of the materials used in the main article.

Abbreviation	HOMO [eV]	LUMO [eV]	Ref.
m-MTDATA	-5.1	-2.0	[1]
TCTA	-5.2	-1.7	[2]
NPB	-5.4	-2.4	[3]
CBP	-6.0	-2.3	[4]
Rubrene	-5.4	-3.2	[5]
Alq_3	-5.6	-3.0	[6]
BCP	-6.4	-2.9	[7]
PO-T2T	-7.5	-3.5	[8]

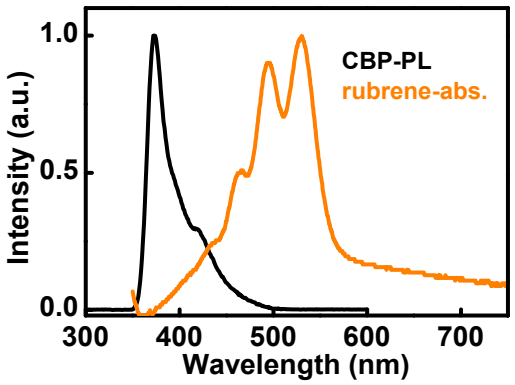

Figure S1 Photoluminescence spectrum of CBP film and absorption spectrum of rubrene film at room temperature.

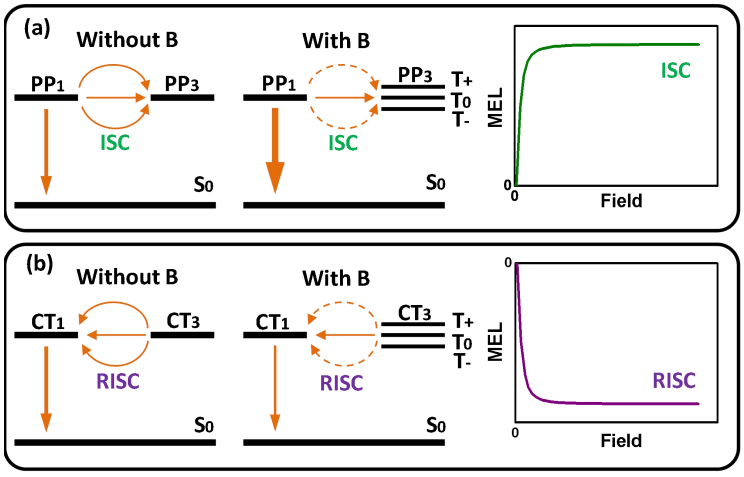

Figure S2 (a) Schematic diagrams of the ISC process from singlet (PP_1) to triplet polaron pairs (PP_3) states in absence and presence of an external magnetic field and ISC-determined MEL fingerprint curve. (b) Schematic diagrams of the RISC process from triplet (CT_3) to singlet charge-transfer (CT_1) states without and with magnetic field and RISC-induced MEL fingerprint curve.

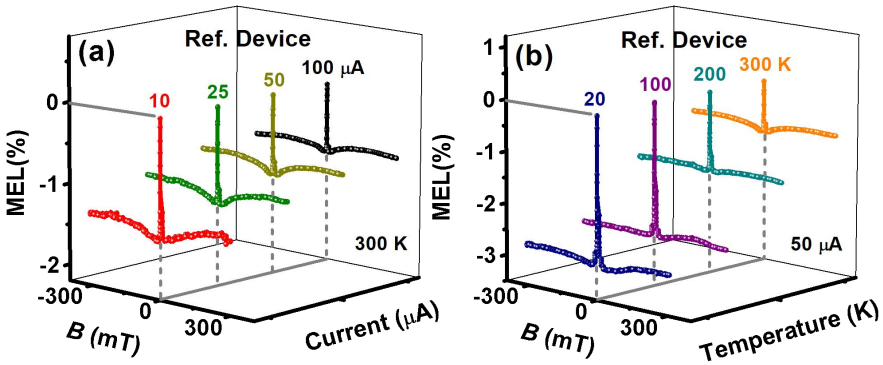

Figure S3 (a) The current dependence of MEL responses in reference device at 300 K. (b) Temperature-dependent MEL responses of reference device at a fixed bias current of 50 μA.

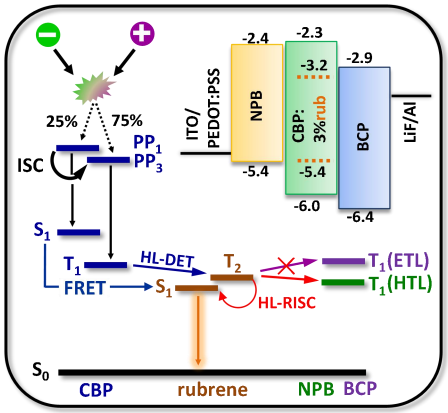

Figure S4 Schematic diagram of microscopic mechanisms in Device 2 and its energy level structure.

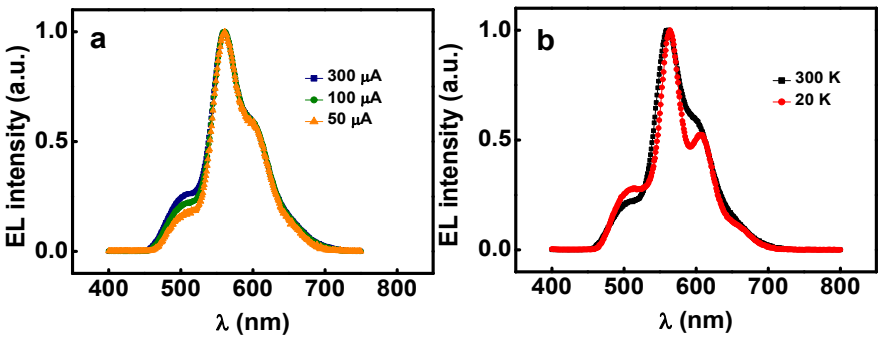

Figure S5 (a) Temperature-dependent normalized EL spectra for Device 4 at a bias current of 100 μA. (b) Current-dependent EL spectra for Device 4 at 300 K.

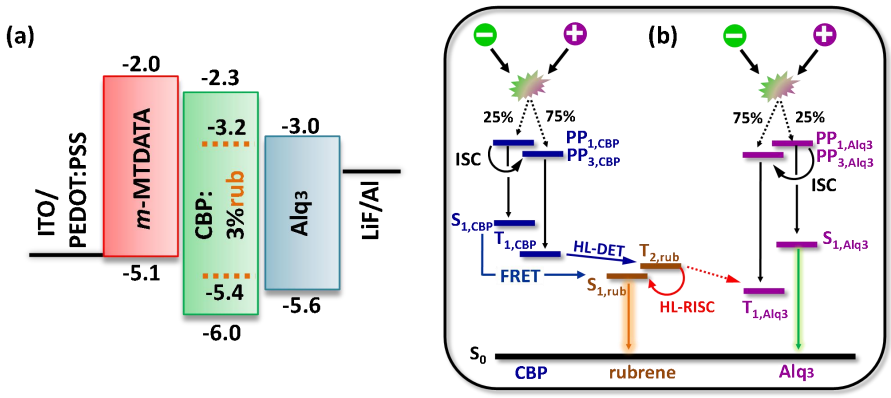

Figure S6 (a) Energy level alignment of Device 4. (b) Schematic diagram of microscopic mechanisms in Device 4.

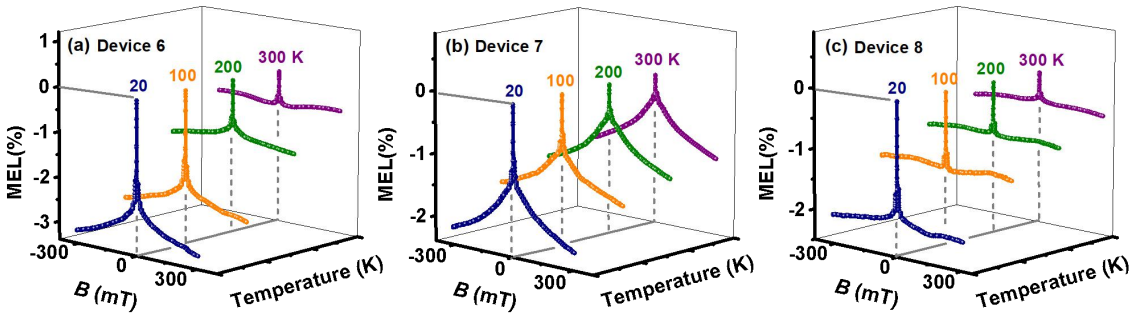

Figure S7 Temperature-dependent MEL responses of (a) Device 6, (b) Device 7, and (c) Device 8.

References

1 N. T. Tierce, C. H. Chen, T. L. Chiu, C. F. Lin, C. J. Bardeen, and J. H. Lee, *Phys. Chem. Chem. Phys.*, 2018, **20**, 27449−27455.

2 J. S. Swensen, E. Polikarpov, A. V. Ruden, L. Wang, L. S. Sapochak, and A. B. Padmaperuma, *Adv. Funct. Mater.*, 2011, **21**, 3250−3258.

3 Q. M. Peng, W. J. Li, S. T. Zhang, P. Chen, F. Li, and Y. G. Ma, *Adv. Opt. Mater.*, 2013, **1**, 362−366.

4 J. Q. Deng, W. Y. Jia, Y. B. Chen, D. Y. Liu, Y. Q. Hu, and Z. H. Xiong, *Sci. Rep.*, 2017, **7**, 44396.

5 D. W. Di, L. Yang, J. M. Richter, L. Meraldi, R. M. Altamimi, A. Y. Alyamani, D. Credgington, K. P. Musselman, J. L. MacManus-Driscoll, and R. H. Friend, *Adv. Mater.*, 2017, **29**, 1605987.

6 Q. M. Peng, N. Gao, W. J. Li, P. Chen, F. Li, and Y. G. Ma, *Appl. Phys. Lett.*, 2013, **102**, 193304.

7 G. R. Fu, L. Liu, W. T. Li, Y. N. He, T. Z. Miao, X. Q. Lü, and H. S. He, *Adv. Opt. Mater.*, 2019, **7**, 1900776.

8 J. H. Lee, S. H. Cheng, S. J. Yoo, H. Shin, J. H. Chang, C. I. Wu, K. T. Wong, and J. J. Kim, *Adv. Funct. Mater.*, 2015, **25**, 361−366.